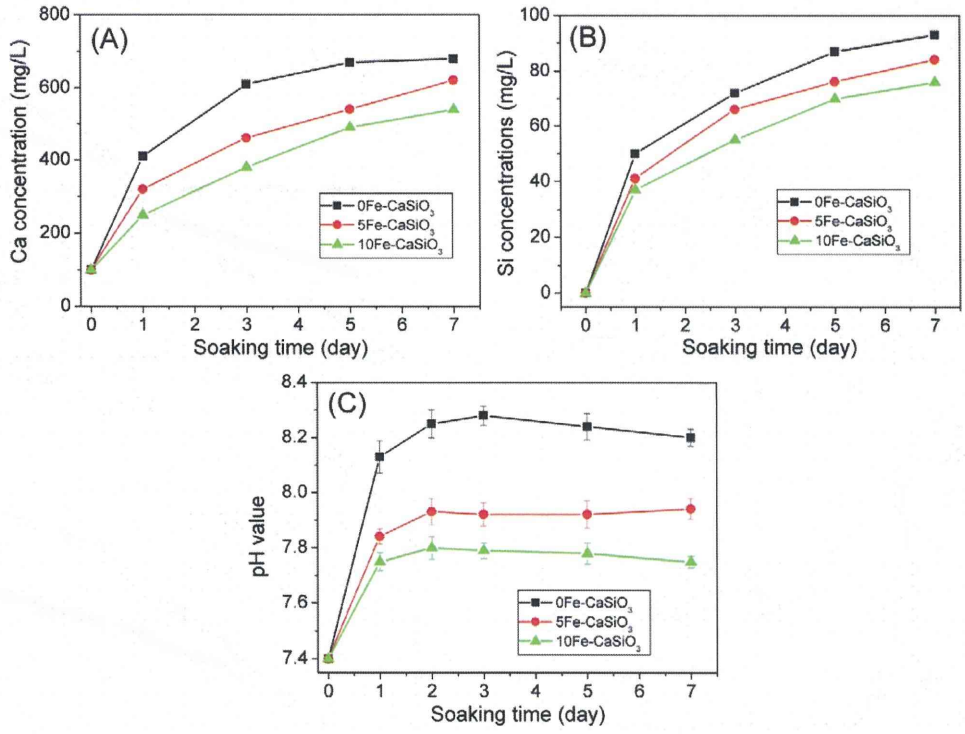


**Figure 6.** Ca (A) and Si (B) ion concentrations in SBF solutions and pH values (C) of SBF solutions after soaking mesoporous Fe-$CaSiO_3$ materials for various time periods.

**Table 3.** The Ca, Si and Fe ion concentrations of mesoporous Fe–$CaSiO_3$ extracts (mg $l^{-1}$).

| | | Extracts concentrations (mg $ml^{-1}$) | | | | |
|---|---|---|---|---|---|---|
| Materials | Ions | Blank | 6.25 | 12.5 | 25 | 50 |
| 0Fe–$CaSiO_3$ | Ca | 72.6 | 73.5 | 78.9 | 86.8 | 96.3 |
| | Si | 0 | 7.8 | 15.8 | 32.0 | 63.1 |
| | Fe | 0 | 0 | 0 | 0 | 0 |
| 5Fe–$CaSiO_3$ | Ca | 72.6 | 73.9 | 76.8 | 80.6 | 89.7 |
| | Si | 0 | 6.2 | 12.2 | 24.5 | 48.6 |
| | Fe | 0 | <1 | <1 | 1.2 | 2.1 |
| 10Fe–$CaSiO_3$ | Ca | 72.6 | 72.7 | 74.5 | 76.4 | 81.1 |
| | Si | 0 | 4.9 | 10.1 | 20.4 | 40.5 |
| | Fe | 0 | <1 | <1 | 1.5 | 2.8 |

drugs, such as antibiotics, for local drug delivery, which is very useful for bone regeneration, because implantation always leads to inflammatory responses and, quite often, to infections [51]. In this study, gentamicin, an antibiotic, was used as a model drug to investigate the drug loading and release behavior of mesoporous Fe–$CaSiO_3$ materials. The gentamicin-loading capacities of the 0Fe–$CaSiO_3$, 5Fe–$CaSiO_3$ and 10Fe–$CaSiO_3$ materials were estimated at 155, 125 and 124 mg $g^{-1}$, respectively. Figure 9 shows the accumulative gentamicin release from mesoporous Fe–$CaSiO_3$ materials in SBF at 37 °C. It can be seen that gentamicin in mesoporous Fe–$CaSiO_3$ materials revealed a sustained release in the SBF solution. The 0Fe–$CaSiO_3$, 5Fe–$CaSiO_3$ and 10Fe–$CaSiO_3$ materials exhibited a similar release behavior throughout the whole study period, with an initial fast release followed by a relatively slow release. Furthermore, the gentamicin release rates from the 0Fe–$CaSiO_3$, 5Fe–$CaSiO_3$ and 10Fe–$CaSiO_3$ materials were close to each other, and the accumulative release of gentamicin was around 85% after 1 week. It suggested that mesoporous Fe–$CaSiO_3$ materials maintained the sustained drug delivery property, and the substitution of Fe for Ca in mesoporous $CaSiO_3$ materials did not change the drug release kinetics.

In this study, the mesopore sizes of the 0Fe–$CaSiO_3$, 5Fe–$CaSiO_3$ and 10Fe–$CaSiO_3$ materials were between 5.3 and 6.2 nm, which are much larger than the size of a gentamicin molecule ($0.52 \times 1.53$ nm) [52], indicating that gentamicin molecules could be loaded in the mesoporous channels. Furthermore, studies demonstrated that silicate-based biomaterials can easily form Si–OH groups on the surface of materials, allowing interacting with gentamicin molecules by hydrogen bonding [53]. On the other hand, the gentamicin release was determined by the mesoporous structure and the interaction between gentamicin and the surface of mesoporous Fe–$CaSiO_3$ materials. The 0Fe–$CaSiO_3$, 5Fe–$CaSiO_3$ and 10Fe–$CaSiO_3$ materials exhibited similar mesoporous structure and surface characteristics, which result in similar gentamicin release kinetics. Therefore, the mesoporous structure of mesoporous Fe–$CaSiO_3$ materials and the Si–OH groups on their surface help to adsorb gentamicin and benefit the sustained release, which indicates their potential as a local drug delivery system for bone tissue regeneration.

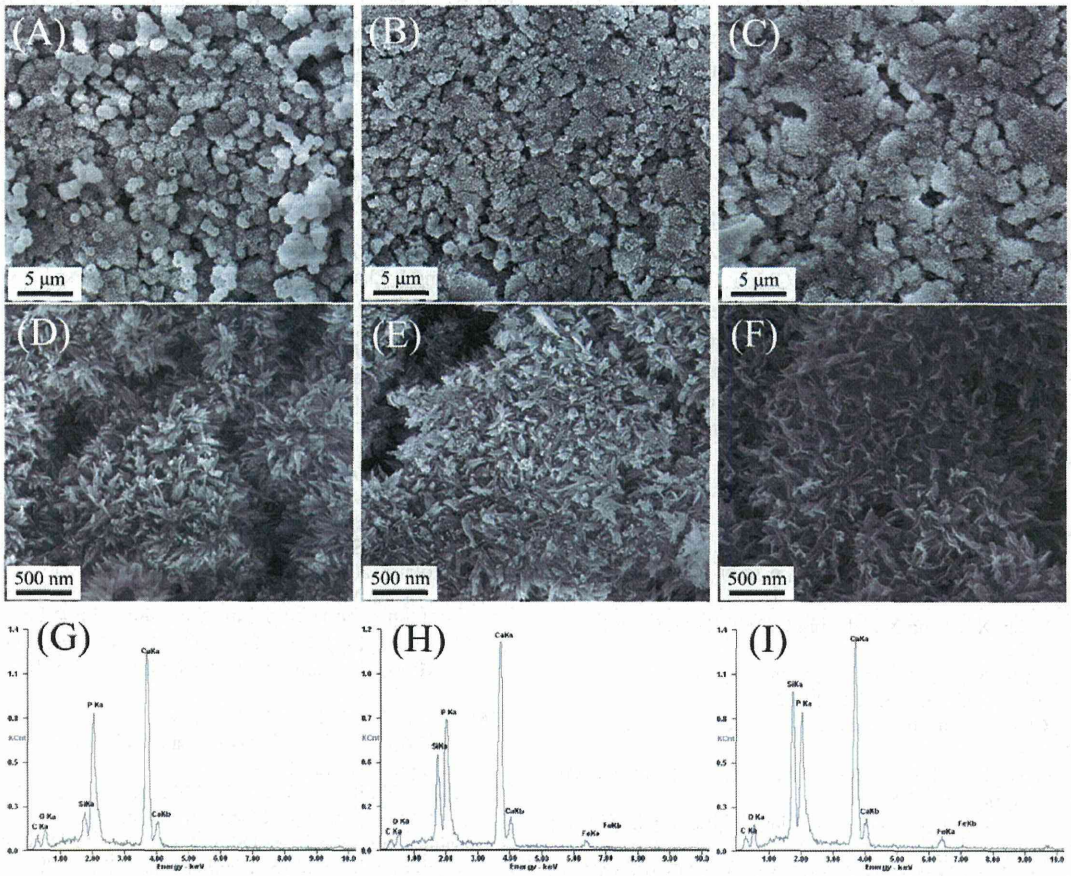


**Figure 7.** SEM images and the corresponding EDS analysis of mesoporous Fe-$CaSiO_3$ materials after soaking in SBF solutions for 3 days ((A), (D) and (G): 0Fe-$CaSiO_3$; (B), (E) and (H): 5Fe-$CaSiO_3$; (C), (F) and (I): 10Fe-$CaSiO_3$).

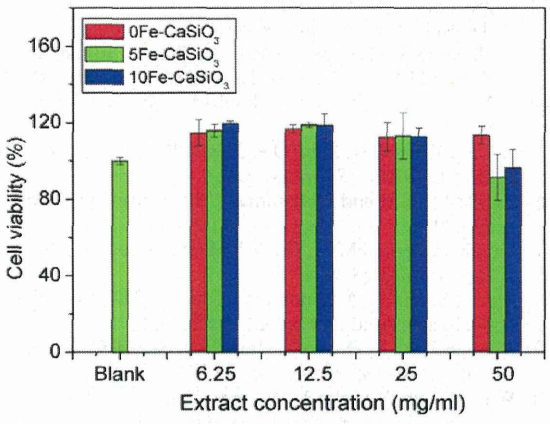


**Figure 8.** The cytotoxic effect of mesoporous Fe-$CaSiO_3$ extracts on MC3T3-E1 cells evaluated by WST-8 assay.

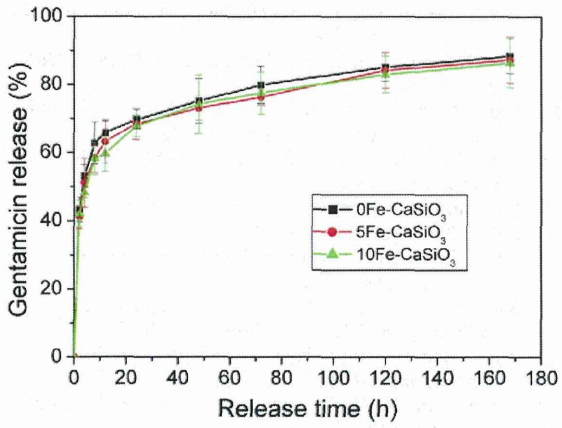


**Figure 9.** Gentamicin release profiles from mesoporous Fe-$CaSiO_3$ materials with different Fe substitution in SBF solution.

## 4. Conclusions

Multifunctional magnetic mesoporous Fe–$CaSiO_3$ materials have been prepared using P123 as a structure-directing agent. The substitution of Fe for Ca in mesoporous $CaSiO_3$ materials did not change their mesoporous structure, but endowed them with magnetic property. The results indicated that mesoporous Fe–$CaSiO_3$ materials exhibited good bioactivity and sustained drug delivery property. Furthermore, magnetic mesoporous Fe–$CaSiO_3$ materials could generate heat in an alternating magnetic field for potential hyperthermia application. Therefore, magnetic mesoporous Fe–$CaSiO_3$ materials have potential for the regeneration of bone defects caused by bone tumors with local drug delivery and magnetic

hyperthermia therapy. Further studies will be conducted to investigate how to fabricate mesoporous Fe–$CaSiO_3$ scaffolds with multifunctionality for bone regeneration.

## Acknowledgments

The authors gratefully acknowledge the support by the Program for Professor of Special Appointment (Eastern Scholar) at Shanghai Institutions of Higher Learning, National Natural Science Foundation of China (no. 51102166), Program for New Century Excellent Talent in University (no. NCET-12-1053), Key Project of Chinese Ministry of Education (no. 212055), Shanghai Pujiang Program (no. 11PJ1407300), Shanghai Shuguang Project (no. 12SG39) and Innovation Program of Shanghai Municipal Education Commission (no. 12ZZ140).

## References

[1] De Aza P N, Guitián F and De Aza S 1997 *Biomaterials* **18** 1285
[2] Xue W, Liu X, Zheng X and Ding C 2005 *Biomaterials* **26** 3455
[3] Fei L, Wang C, Xue Y, Lin K, Chang J and Sun J 2012 *J. Biomed. Mater. Res.* B **100B** 1237
[4] Ni S, Chang J and Chou L 2006 *J. Biomed. Mater. Res.* A **76A** 196
[5] Yan X, Huang X, Yu C, Deng H, Wang Y and Zhang Z 2006 *Biomaterials* **27** 3396
[6] Ostomel T A, Shi Q, Tsung C K, Liang H and Stucky G D 2006 *Small* **2** 1261
[7] Li X, Shi J, Zhu Y, Shen W, Li H, Liang J and Gao J 2007 *J. Biomed. Mater. Res.* B **83B** 431
[8] Xia W and Chang J 2008 *Micropor. Mesopor. Mater.* **108** 345
[9] Wu C, Chang J and Fan W 2012 *J. Mater. Chem.* **22** 16801
[10] Wei J, Chen F, Shin J, Hong H, Dai C, Su L and Liu C 2009 *Biomaterials* **30** 1080
[11] Zhu H, Wu B, Feng X and Chen J 2011 *J. Biomed. Mater. Res.* B **98B** 330
[12] Fan Y, Huang S, Jiang J, Li G, Yang P, Lian H, Cheng Z and Lin J 2011 *J. Colloid Interface Sci.* **357** 280
[13] Ariga K, Vinu A, Yamauchi Y, Ji Q and Hill J P 2012 *Bull. Chem. Soc. Japan* **85** 1
[14] He Q and Shi J 2011 *J. Mater. Chem.* **21** 5845
[15] Derby B 2012 *Science* **338** 921
[16] Zhu Y, Li X, Yang J, Wang S, Gao H and Hanagata N 2011 *J. Mater. Chem.* **21** 9208
[17] Salinas A J, Shruti S, Malavasi G, Menabue L and Vallet-Regí M 2011 *Acta Biomater.* **7** 3452
[18] Wu C, Ramaswamy Y, Kwik D and Zreiqat H 2007 *Biomaterials* **28** 3171
[19] Ramaswamy Y, Wu C, Zhou H and Zreiqat H 2008 *Acta Biomater.* **4** 1487
[20] Zreiqat H, Ramaswamy Y, Wu C, Paschalidis A, Lu Z, James B, Birke O, McDonald M, Little D and Dunstan C R 2010 *Biomaterials* **31** 3175
[21] Chen X, Ou J, Wei Y, Huang Z, Kang Y and Yin G 2010 *J. Mater. Sci. Mater. Med.* **21** 1463
[22] Wu C, Ramaswamy Y, Soeparto A and Zreiqat H 2008 *J. Biomed. Mater. Res. A* **86A** 402
[23] Lu J *et al* 2012 *Micropor. Mesopor. Mater.* **163** 221
[24] Zhu Y, Zhu M, He X, Zhang J and Tao C 2013 *Acta Biomater.* **9** 6723
[25] Yamasaki K and Hagiwara H 2009 *Toxicol. Lett.* **191** 211
[26] Wu Y, Jiang W, Wen X, He B, Zeng X, Wang G and Gu Z 2010 *Biomed. Mater.* **5** 015001
[27] Panseri S, Cunha C, D'Alessandro T, Sandri M, Russo A, Giavaresi G, Marcacci M, Hung C T and Tampieri A 2012 *PLoS ONE* **7** e38710
[28] Meng J, Zhang Y, Qi X, Kong H, Wang C, Xu Z, Xie S, Gu N and Xu H 2010 *Nanoscale* **2** 2565
[29] Parsons A J, Evans M, Rudd C D and Scotchford C A 2004 *J. Biomed. Mater. Res.* A **71A** 283
[30] Bock N, Riminucci A, Dionigi C, Russo A, Tampieri A, Landi E, Goranov V A, Marcacci M and Dediu V 2010 *Acta Biomater.* **6** 786
[31] Zeng X, Hu H, Xie L, Lan F, Jiang W, Wu Y and Gu Z 2012 *Int. J. Nanomed.* **7** 3365
[32] Martín-Saavedra F M, Ruíz-Hernández E, Boré A, Arcos D, Vallet-Regí M and Vilaboa N 2010 *Acta Biomater.* **6** 4522
[33] Murakami S, Hosono T, Jeyadevan B, Kamitakahara M and Ioku K 2008 *J. Ceramic Soc. Japan* **116** 950
[34] Kawashita M, Iwahashi Y, Kokubo T, Yao T, Hamada S and Shinjo T 2004 *J. Ceram. Soc. Japan* **112** 373
[35] Julián-López B, Boissière C, Chanéac C, Grosso D, Vasseur S, Miraux S, Duguet E and Sanchez C 2007 *J. Mater. Chem.* **17** 1563
[36] Lee H, Kim S, Choi B H, Park M T, Lee J, Jeong S Y, Choi E K, Lim B U, Kim C and Park H J 2011 *Int. J. Hyperthermia* **27** 698
[37] Hu M, Belik A A, Imura M, Mibu K, Tsujimoto Y and Yamauchi Y 2012 *Chem. Mater.* **24** 2698
[38] Zhu Y, Shang F, Li B, Dong Y, Liu Y, Lohe M R, Hanagata N and Kaskel S 2013 *J. Mater. Chem.* B **1** 1279
[39] Wu C, Fan W, Zhu Y, Gelinsky M, Chang J, Cuniberti G, Albrecht V, Friis T and Xiao Y 2011 *Acta Biomater.* **7** 3563
[40] Kokubo T and Takadama H 2006 *Biomaterials* **27** 2907
[41] Zhu Y and Kaskel S 2009 *Micropor. Mesopor. Mater.* **118** 176
[42] Siriphannon P, Kameshima Y, Yasumor A, Okada K and Hayashi S 2002 *J. Eur. Ceram. Soc.* **22** 511
[43] Gu J, Dong X, Elangovan S P, Li Y, Zhao W, Iijima T, Yamazaki Y and Shi J 2012 *J. Solid State Chem.* **186** 208
[44] Li X, Wang X P, Hua Z L and Shi J L 2008 *Acta Mater.* **56** 3260
[45] Chen Y, Chen H R, Zeng D P, Tian Y B, Chen F, Feng J W and Shi J L 2010 *ACS Nano* **4** 6001
[46] Kumar C S S R and Mohammad F 2011 *Adv. Drug Deliv. Rev.* **63** 789
[47] Valerio P, Pereira M M, Goes A M and Leite M F 2004 *Biomaterials* **25** 2941
[48] Maeno S, Niki Y, Matsumoto H, Morioka H, Yatabe T and Funayama A 2005 *Biomaterials* **26** 4847
[49] Kokubo T, Ito S, Huang Z, Hayashi T, Sakka S and Kitsugi T 1990 *J. Biomed. Mater. Res.* **24** 331
[50] Wu C T, Fan W, Gelinsky M, Xiao Y, Simon P, Schulze R, Doert T, Luo Y X and Cuniberti G 2011 *Acta Biomater.* **7** 1797
[51] Vallet-Regi M 2006 *Dalton Trans.* **44** 5211
[52] Doadrio A L, Sousa E M B, Doadrio J C, Pariente J P, Barba I I and Vallet-Regi M 2004 *J. Control Release* **97** 125
[53] Xia W and Chang J 2006 *J. Control Release* **110** 522

Society For Biomaterials

# Calcium-incorporated titanium surfaces influence the osteogenic differentiation of human mesenchymal stem cells

**Rumi Sawada,[1] Ken Kono,[1] Kazuo Isama,[2] Yuji Haishima,[1] Atsuko Matsuoka[1]**

[1]Division of Medical Devices, National Institute of Health Sciences, Tokyo, Japan
[2]Division of Environmental Chemistry, National Institute of Health Sciences, Tokyo, Japan

Received 21 September 2012; accepted 13 December 2012
Published online 11 February 2013 in Wiley Online Library (wileyonlinelibrary.com). DOI: 10.1002/jbm.a.34566

**Abstract:** In this study, a titanium surface was chemically modified with calcium ions and assessed for its influence on osteogenic differentiation and molecular responses of human mesenchymal stem cells (hMSCs). Titanium disks were treated with NaOH (NaOH treatment), NaOH + $CaCl_2$ ($CaCl_2$ treatment), or NaOH + $Ca(OH)_2$ ($Ca(OH)_2$ treatment). $Ca(OH)_2$ treatment caused significantly greater calcium incorporation onto the titanium surface and apatite formation than $CaCl_2$ treatment. The morphology of hMSCs differed on $CaCl_2$- and $Ca(OH)_2$-treated disks. The osteopontin (OPN) expression in hMSCs cultured on $CaCl_2$-treated titanium was significantly higher than that in cells cultured on NaOH-treated disks; OPN expression was significantly higher in cells cultured on $Ca(OH)_2$-treated disks than on un-, NaOH-, and $CaCl_2$-treated disks. Osteocalcin (OCN) protein expression in hMSCs cultured on $Ca(OH)_2$-treated disks was significantly higher than that on all the other disks. Comparative expression profiling by DNA microarray and pathway analyses revealed that calcium modification of the titanium surface induced integrin β3 after OPN upregulation and promoted Wnt/β-catenin signaling in hMSCs. In addition, $Ca(OH)_2$ treatment upregulated the expression of bone morphogenetic protein 2, cyclooxygenase 2, and parathyroid hormone-like hormone in comparison to $CaCl_2$ treatment. These observations suggest that calcium-modified titanium surfaces affect osteogenic differentiation in hMSCs and that $Ca(OH)_2$ treatment induced osteogenic differentiation in hMSCs, whereas $CaCl_2$ treatment had a limited effect. © 2013 Wiley Periodicals, Inc. J Biomed Mater Res Part A: 101A: 2573–2585, 2013.

**Key Words:** surface modification, titanium, calcium, stem cell, osteogenesis, gene expression

**How to cite this article:** Sawada R, Kono K, Isama K, Haishima Y, Matsuoka A. 2013. Calcium-incorporated titanium surfaces influence the osteogenic differentiation of human mesenchymal stem cells. J Biomed Mater Res Part A 2013:101A:2573–2585.

## INTRODUCTION

Titanium is widely used in orthopedic and dental implants due to its corrosion and wear resistance, durability, and biocompatible interface. The topography of titanium implants plays a major role in cell–material interaction. Several studies have shown that surface modifications influence protein adsorption,[1,2] cell–substrate interactions,[3] cell adhesion,[3–5] cell morphology,[5,6] osteogenic differentiation,[5,7–10] and, consequently, the tissue integration of titanium implants.[11,12]

The nanoscale and microscale surface roughness of titanium has been reported to increase osteogenic differentiation in osteoblasts cultured on titanium surfaces[7,9–12] and promote osteogenic differentiation in human mesenchymal stem cells (hMSCs) in the presence of osteogenic supplements.[8] Osteoblast response has also been reported to be modulated by a modified microstructured titanium surface with increased wettability due to a polyelectrolyte thin film coating.[13] Titanium nanopores also affect osteogenic differentiation and hMSC cell morphology.[5] Integrin is critical for the responses of osteoblasts[4,10,14] and hMSCs[5] to some titanium surface modifications. Gene expression studies have shown an increase in the expression of the osteoinductive genes RUNX2, osterix, alkaline phosphatase, bone sialoprotein, and osteocalcin (OCN) in osteoblasts[6,15] and hMSCs[16,17] grown on micro- and nanoroughened surfaces in the presence of osteogenic supplements.

Alkali- and heat-treated titanium forms a bone-like apatite surface layer in the body and bonds to the bone via this layer.[18–22] In addition to chemical and thermal treatments, the porous structure of titanium contributes to its biocompatibility[23] and bone formation[24] *in vivo*. Fluoride ion modification of a $TiO_2$ grit-blasted surface enhances osteoblastic differentiation in hMSCs in the presence of osteogenic supplements.[25] Calcium ion incorporation into a titanium surface by $CaCl_2$ treatment yields slightly better apatite formation than alkali (NaOH) treatment *in vitro*,[26] but the influence of calcium ion modifications of titanium surfaces on osteogenic differentiation of hMSCs has not been explored.

hMSCs are pluripotent and can differentiate into cells of mesodermal origin, for example, bone, cartilage, adipose,

**Correspondence to:** R. Sawada; e-mail: rsawada@nihs.go.jp
Contract grant sponsor: Health and Labour Sciences Research Grants for Research on Regulatory Science of Pharmaceuticals and Medical Devices from the Ministry of Health, Labour and Welfare of Japan; contract grant numbers: H22-IYAKU-IPPAN-009, H24-IYAKU-SHITEI-018

and muscle cells.[27–31] hMSCs also have the capacity to differentiate into myocytes,[32,33] hepatocytes,[27,34] and neural cells.[29] hMSCs are currently being used with biomedical materials in several clinical studies on bone regeneration.

We aimed to evaluate the influence of $CaCl_2$- or $Ca(OH)_2$-modified titanium surfaces on osteogenic differentiation and molecular responses in hMSCs. We examined the amount of calcium ion incorporation and apatite formation on $CaCl_2$- and $Ca(OH)_2$-treated surfaces. We investigated the morphology, proliferation, and osteogenic differentiation of hMSCs cultured on the chemically modified titanium. To definitively conclude whether incorporation of calcium ions on a titanium surface induces osteogenic differentiation in hMSCs, osteogenic supplements were not used in this study. Whole genome expression analysis provided a comprehensive understanding of the mechanism of osteogenic induction by chemically modified titanium.

## MATERIALS AND METHODS

### Chemical treatment of titanium disks

Titanium disks (grade II commercially pure titanium, 33.5 mm diameter, 2-mm thick) were supplied by Nakashima Medical Co. (Okayama, Japan). They contain over 99.3075% of titanium, and their surface roughness (Ra) is 0.4 μm. NaOH treatment was performed by soaking the disks in 5.0 mol/L NaOH aqueous solution at 60°C for 24 h and then washing gently with distilled water. $CaCl_2$ or $Ca(OH)_2$ treatments were performed by soaking the NaOH-treated disks in 0.1 mol/L $CaCl_2$ or 0.01 mol/L $Ca(OH)_2$ at 60°C for 24 h and then gently washing with distilled water. Untreated titanium disks served as controls.

### Scanning electron microscopy

The topography of the chemically modified titanium disks was characterized by Scanning electron microscopy (SEM) performed with a JSM-5800 microscope (JEOL, Tokyo, Japan). Images were recorded with 15 kV accelerating voltage.

### Calcium ion incorporation and apatite formation

To investigate apatite formation on the titanium surface, untreated or chemically modified disks were soaked in Hanks' balanced salt solution that included calcium and magnesium (Life Technologies Co., Carlsbad, CA) for 7 days at 37°C. The solution was changed every 2 days.

The incorporated calcium ions were dissolved in nitric acid and their concentration was measured by Agilent 7500ce ORS ICP-MS (inductively coupled plasma mass spectrometry; Agilent, Santa Clara, CA) in helium collision mode with monitoring at $m/z$ 43.

### Cell culture

hMSCs derived from bone marrow were purchased from Lonza (Walkersville, MD). The hMSCs were cultured in MSCGM BulletKit, a mesenchymal stem cell basal medium with mesenchymal cell growth supplement, L-glutamine, and gentamycin/amphotericin-B (Lonza Walkersville, MD), at 37°C under a 5% $CO_2$ atmosphere. The medium was changed every 3 days. The cells were detached by mild treatment with trypsin/ethylenediaminetetraacetic acid solution for hMSCs (Lonza Walkersville, MD) and subcultured when they were just subconfluent (approximately 80–90% confluence). Cell passages 2–4 were used for experiments. hMSCs were cultured on each surface-modified titanium disk for 1, 4, 7, and 28 days.

### Cell morphology and immunofluorescence staining

To analyze the morphology of hMSCs cultured on the chemically modified titanium disks, the cells were stained with CellTracker (Lonza) according to the manufacturer's protocol.

To examine the expression of OCN, cells stained with CellTracker were fixed with 4% paraformaldehyde in phosphate buffered saline (PBS) for 15 min at room temperature and permeabilized with a blocking solution [10% normal donkey serum (Jackson ImmunoResearch Laboratories, Baltimore, PA), 0.1% Triton X-100, and 0.01% $NaN_3$ in PBS]. The cells were stained with anti-OCN antibody (Abcam, Cambridge, MA) in blocking solution without Triton X-100 for 16 h at 4°C for primary staining and were secondarily stained with Alexa Fluor 647-conjugated donkey anti-mouse antibody (Jackson ImmunoResearch Laboratories) for 30 min at room temperature.

Images were collected and analyzed by confocal microscopy (FLUOVIEW FV1000; Olympus, Tokyo, Japan).

### Cell proliferation

The proliferation of hMSCs on titanium disks for 7 days was determined by using a cell proliferation assay reagent, TetraColor ONE (Seikagaku Co., Tokyo, Japan). Cultures were incubated for 2 h in medium containing the reagent. The absorbance was read at 450 nm (reference at 600 nm) on a plate reader (SH-9000, Corona Electric Co., Ibaraki, Japan).

### Preparation of total RNA and real-time polymerase chain reaction

hMSCs were seeded on untreated and chemically modified titanium disks in 35 mm culture dishes at an initial seeding density of $1.2 \times 10^4$ cells/cm$^2$ and cultured for 7 days before evaluating transcript expression of osteopontin (OPN), OCN, and glyceraldehyde-3-phosphate dehydrogenase (GAPDH). The housekeeping gene GAPDH was used as a control. Total RNA was extracted from hMSCs with the RNeasy Mini Kit (QIAGEN, Valencia, CA). Total RNA was eluted in RNase-free water and quantified on a NanoDrop 1000 spectrophotometer (Thermo Scientific, Wilmington, DE). Total RNA was reverse transcribed with the SuperScript III First-Strand Synthesis System for real-time polymerase chain reaction (RT-PCR; Life Technologies Co., Carlsbad, CA). Amplification of OPN, OCN, and GAPDH was performed with LightCycler Primer Sets (Roche Applied Science, Basel, Switzerland) and LightCycler Fast Start DNA Master SYBR Green I (Roche Applied Science) in a Roche LightCycler instrument (software version 4.0).

### Microarray analysis

Whole genome expression was analyzed after 7-day culture of hMSCs on chemically modified titanium disks. Total RNA

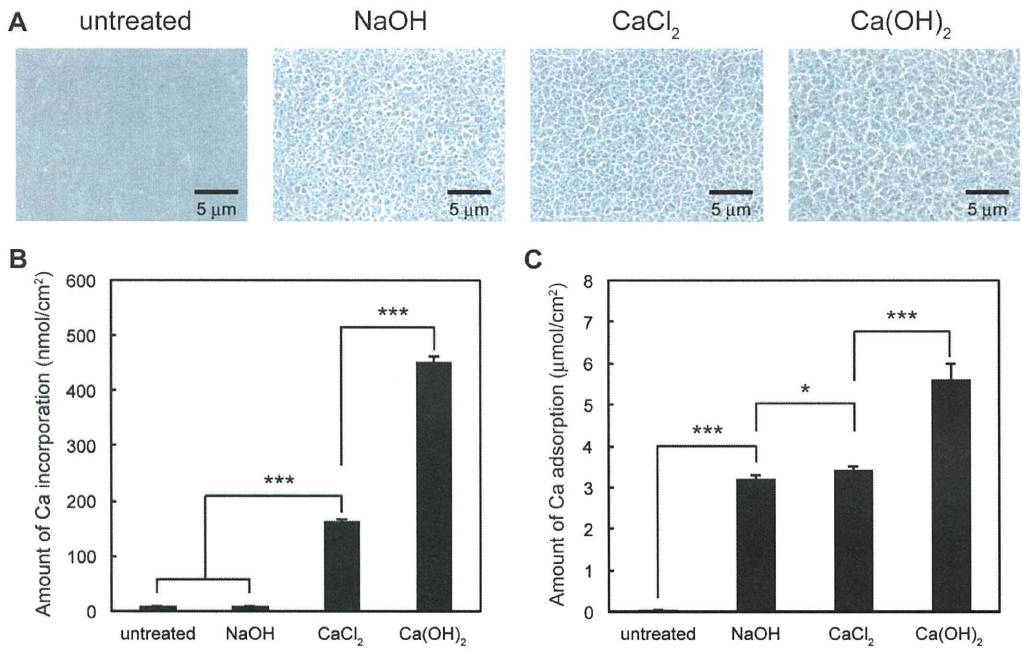


**FIGURE 1.** SEM images of the surface of untreated, NaOH-, NaOH + $CaCl_2$ ($CaCl_2$)-, and NaOH + $Ca(OH)_2$ ($Ca(OH)_2$)-treated titanium disks (A). Images are representative of three independent experiments. The amount of $Ca^{2+}$ incorporation into the chemically modified titanium disks (B; left) and the amount of $Ca^{2+}$ adsorption onto the modified disks after soaking in Hanks' balanced salt solution including calcium and magnesium at 37°C for 7 days (B; right) were measured by ICP-MS ($n = 3$). Significant differences between groups are shown as $^{*}p < 0.05$ and $^{***}p < 0.001$.

quantity and quality were assessed on an Agilent 2100 Bioanalyzer (Agilent, Santa Clara, CA); 100 ng of total RNA was used to generate biotin-modified amplified RNA (aRNA) with the GeneChip 3'IVT Express Kit (Affymetrix, Santa Clara, CA). Reverse transcription of first-strand complementary DNA (cDNA) with a T7 promoter sequence was performed with T7 oligo(dT) primer. Second-strand cDNA synthesis was used to convert the single-stranded cDNA into a double-stranded DNA template. The reaction employed DNA polymerase and RNase H to simultaneously degrade the RNA and synthesize second-strand cDNA. *In vitro* transcription of biotin-modified aRNA with IVT Labeling Master Mix generated multiple copies of biotin-modified aRNA from the double-stranded cDNA templates. The aRNA was purified and quantified; after fragmentation, it was hybridized to the GeneChip Human Genome U133 Plus 2.0 Array (Affymetrix). The arrays were stained with phycoerythrin and washed at the GeneChip Fluidics Station 450 (Affymetrix). The microarrays were scanned and data extracted using GeneChip scanner 3000 7G (Affymetrix), image analysis was performed using the Affymetrix GeneChip Command Console Software and digitized using Affymetrix Expression Console.

### Data processing and pathway analysis

Data analysis was performed with GeneSpring GX 11.0 software (Agilent Technologies, Santa Clara, CA). Raw data were normalized to the 50th percentile per chip and the median per gene. Normalized means for the four kinds of titanium disks (un-, NaOH-, $CaCl_2$-, or $Ca(OH)_2$-treated) were generated for the experimental interpretation. Differentially expressed genes were selected and flagged for further analysis. To determine whether particular osteogenic differentiation functions were significantly overrepresented, the data set was analyzed using Ingenuity Pathway Analysis (IPA) 9.0 (Ingenuity Systems, Redwood City, CA).

### Statistical analysis

All results are shown as means ± SD. Significance was evaluated by the Student's *t* test.

## RESULTS

### Surface characterization of chemically modified titanium disks

Titanium disks were treated with NaOH (NaOH treatment), NaOH + $CaCl_2$ ($CaCl_2$ treatment), and NaOH + $Ca(OH)_2$ ($Ca(OH)_2$ treatment; see Materials and methods section). SEM demonstrated a porous network structure formed on the surface of the disks after chemical treatment [Fig. 1(A)]. There were no significant differences between the chemically treated surfaces.

### Calcium ion incorporation and apatite formation on the titanium surface

We measured the amount of calcium ion incorporation on the surface of the modified titanium disks [Fig. 1(B)]. As expected, no calcium ions were incorporated into the untreated or NaOH-treated disks. Significantly more calcium ions were incorporated into the $Ca(OH)_2$-treated disks than the $CaCl_2$-treated disks.

To investigate the effects of chemical treatments on apatite formation on the titanium surface, the disks were

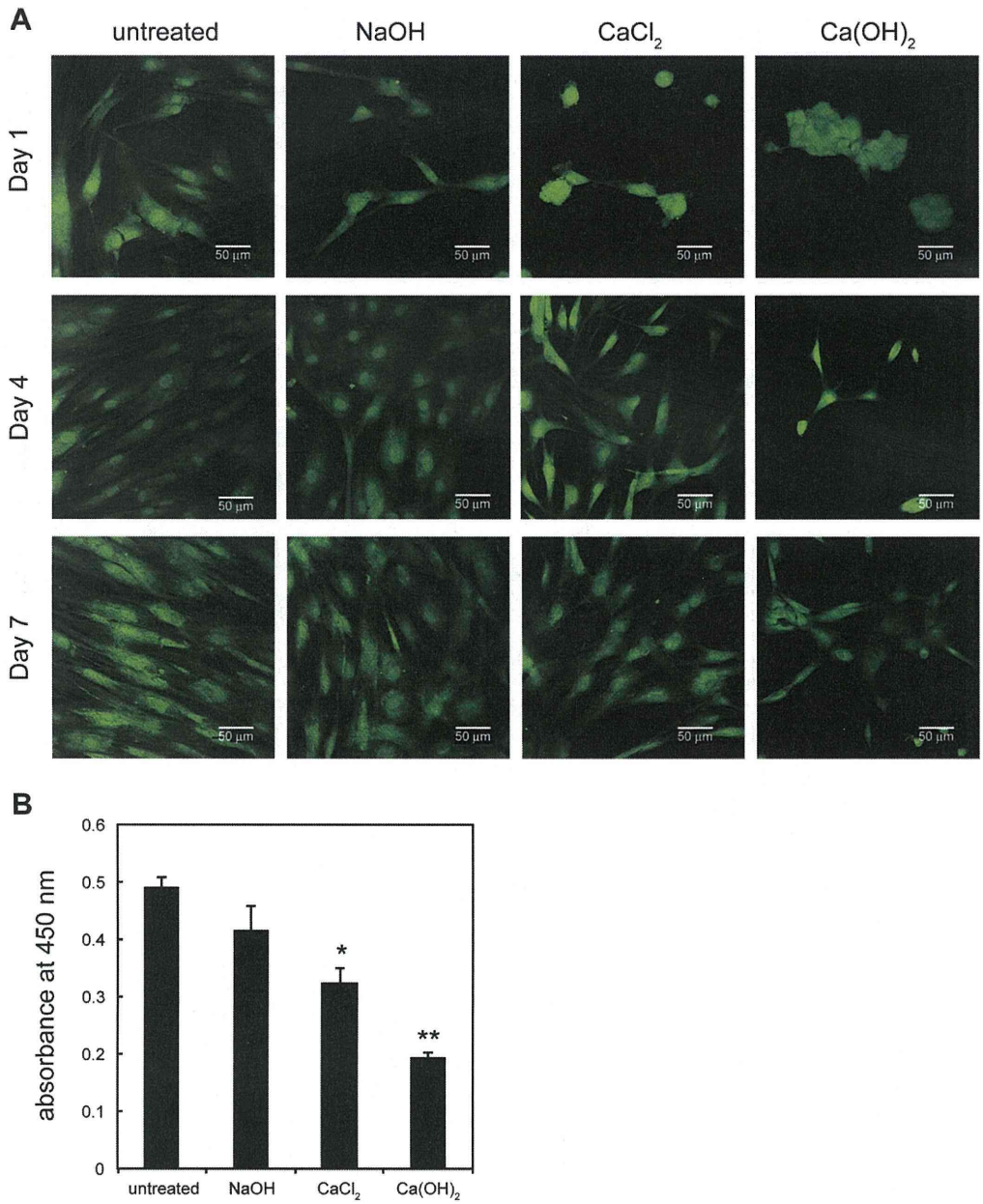


**FIGURE 2.** Confocal microscopy of hMSCs cultured on untreated, NaOH, $CaCl_2$, and $Ca(OH)_2$ treated titanium disks for 1, 4, and 7 days (A). Images are representative of five independent experiments. Cells were stained with CellTrackerTM Green Fluorescent Probe (Lonza). Proliferation of hMSCs for 7 days was determined with the cell proliferation assay reagent TetraColor One (B). The optical density of each well was measured at 450 nm ($n = 3$). Significant differences in comparison to untreated titanium are shown as $^*p < 0.05$ and $^{**}p < 0.01$. [Color figure can be viewed in the online issue, which is available at wileyonlinelibrary.com.]

soaked in Hanks' Balanced Salt Solution for 7 days. The amount of $Ca^{2+}$ on titanium disks treated with NaOH, $CaCl_2$, and Ca(OH) was directly correlated with apatite formation. Apatite formation was slightly but significantly greater on $CaCl_2$-treated disks than on NaOH-treated disks [Fig. 1(C)]. Furthermore, $Ca(OH)_2$-treated titanium disk caused significantly greater apatite formation than the NaOH- and $CaCl_2$-treated disks [Fig. 1(C)].

### Cell morphology and proliferation

To understand cell adhesion, we investigated the morphologies of hMSCs cultured on chemically modified titanium disks. We labeled the cells with CellTracker (Lonza) and observed at 1, 4, and 7 days after seeding. Confocal microscopy revealed cells on the modified disks showed smaller spread areas 1 day after seeding, although cells on the untreated disks exhibited normal cell morphology [Fig. 2(A)

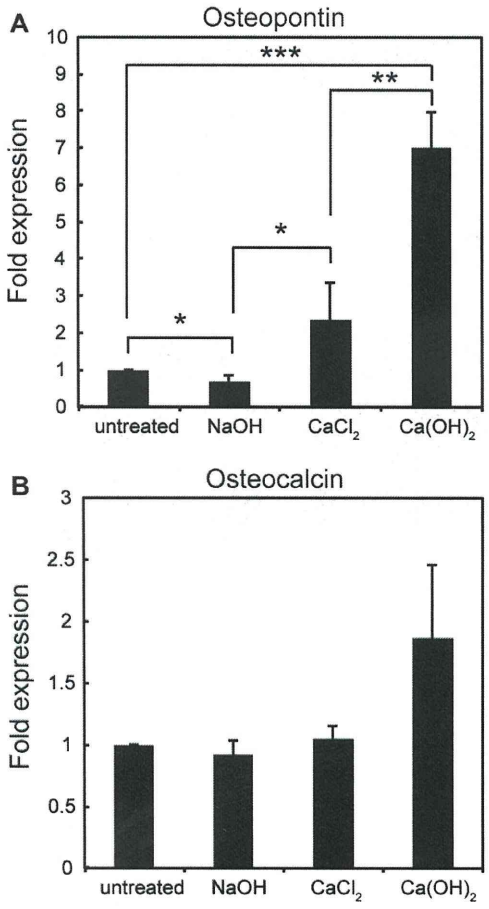


**FIGURE 3.** Relative expression of osteopontin (A) and osteocalcin (B) were analyzed by real-time PCR at 7 days after hMSC seeding ($n = 3$). The value was normalized to GAPDH. Significant differences between groups are shown as $*p < 0.05$, $**p < 0.01$, and $***p < 0.001$.

upper panels]. Cells grown on $CaCl_2$- or $Ca(OH)_2$-treated disks were round in shape. Four days after seeding, the cells on NaOH- or $CaCl_2$-treated disks were comparable to cells cultured on untreated disks, whereas the cells on the $Ca(OH)_2$-treated disk were not. hMSCs on $Ca(OH)_2$-treated disks were comparable in shape at 7 days after seeding [Fig. 2(A) middle and lower panels]. hMSC proliferation for 7 days was also investigated. Culture on chemically modified titanium surfaces decreased hMSC cell numbers [Fig. 2(B)].

### Cell differentiation and quantitative real-time PCR

To investigate the osteogenic differentiation of hMSCs cultured on chemically modified titanium disks, OPN and OCN transcripts were characterized by real-time PCR after culture for 7 days (Fig. 3). The transcript levels of OPN in hMSCs cultured on $CaCl_2$-treated titanium disks were significantly higher than those on NaOH-treated disks [Fig. 3(A)]. OPN expression was significantly greater on $Ca(OH)_2$-treated disks than on un-, NaOH-, and $CaCl_2$-treated disks [Fig. 3(A)]. OCN expression on $Ca(OH)_2$-treated disks was slightly higher than on the other treated disks [Fig. 3(B)].

We also examined OCN protein expression by immunofluorescence. We observed hMSCs cultured on chemically modified titanium for 7, 14, 21 days (data not shown), and 28 days [Fig. 4(A)]. Although we did not detect expression on all cells until 21 days after seeding (data not shown), only hMSCs on the $Ca(OH)_2$-treated disks showed OCN expression 28 days after seeding [Fig. 4(B)]. The fluorescence intensity of hMSCs cultured on $Ca(OH)_2$-treated titanium was significantly stronger than on the other treated disks [Fig. 4(C)].

### Microarray and pathway analysis

To investigate the mechanism of osteogenic induction in hMSCs by chemically modified titanium, we performed DNA microarray analysis. We analyzed mRNA extracted from hMSCs cultured on chemically modified titanium for 7 days. The top 30 genes significantly upregulated on treated versus untreated titanium disks are summarized in Tables I–III. A significant change was defined as a difference of more than twofold relative to the control. Differentially expressed genes significantly upregulated on NaOH versus nontreated disks are shown in Table I. Interleukin 6 receptor (IL6R) increases osteoblast differentiation, and integrin, beta 1 (ITGB1) plays a critical role in the process; both were significantly upregulated on NaOH-treated disks (Table I). Genes significantly upregulated by $CaCl_2$ or $Ca(OH)_2$ treatments versus the untreated control are shown in Tables II and III. SPP1 (OPN) and MMP13 (matrix metallopeptidase 13), involved in normal bone remodeling,[35] and ectonucleotide pyrophosphatase (ENPP1) increase osteoblast differentiation[36]; all were significantly upregulated by $CaCl_2$ or $Ca(OH)_2$ treatment (Tables II and III). In addition, $Ca(OH)_2$ treatment significantly upregulated the expression of IL6R and integrin, alpha 2 (ITGA2), which plays a critical role in osteoblast differentiation, bone morphogenetic protein 2 (BMP2), and parathyroid hormone-like hormone (PTHLH), which also affects osteoblast differentiation (Table III). To differentiate the effect of different calcium surface treatments on gene expression, we compared gene profiles in hMSCs cultured on $CaCl_2$ and on $Ca(OH)_2$. The expression of 94 genes in hMSCs cultured on $Ca(OH)_2$ disks were upregulated more than twofold in comparison to cells grown on $CaCl_2$ (data not shown). Six of these genes significantly ($p = 3.96 \times 10^{-4}$) overlapped with the genes associated with "formation of bone" in the IPA. The genes were SPP1, PTHLH, FGF1 (fibroblast growth factor 1), BMP2, PTGS1 (cyclooxygenase 1), and PTGS2 (cyclooxygenase 2; Cox2) (Table IV).

To determine the significance of the effects of different titanium treatments on osteogenic differentiation in hMSCs, we used IPA. Differentially expressed genes that were significantly influenced by NaOH, $CaCl_2$, or $Ca(OH)_2$ treatment were compared with untreated controls in the canonical pathway defined by IPA in osteoblast and are shown in Figures 5–7. Genes that were not detected in untreated controls, but were detected in hMSCs cultured on chemically modified titanium are represented as "induced genes" in these figures. Genes that were detected in untreated controls but not in hMSCs grown on chemically modified titanium are indicated as "suppressed genes". The NaOH-treated titanium surface induced

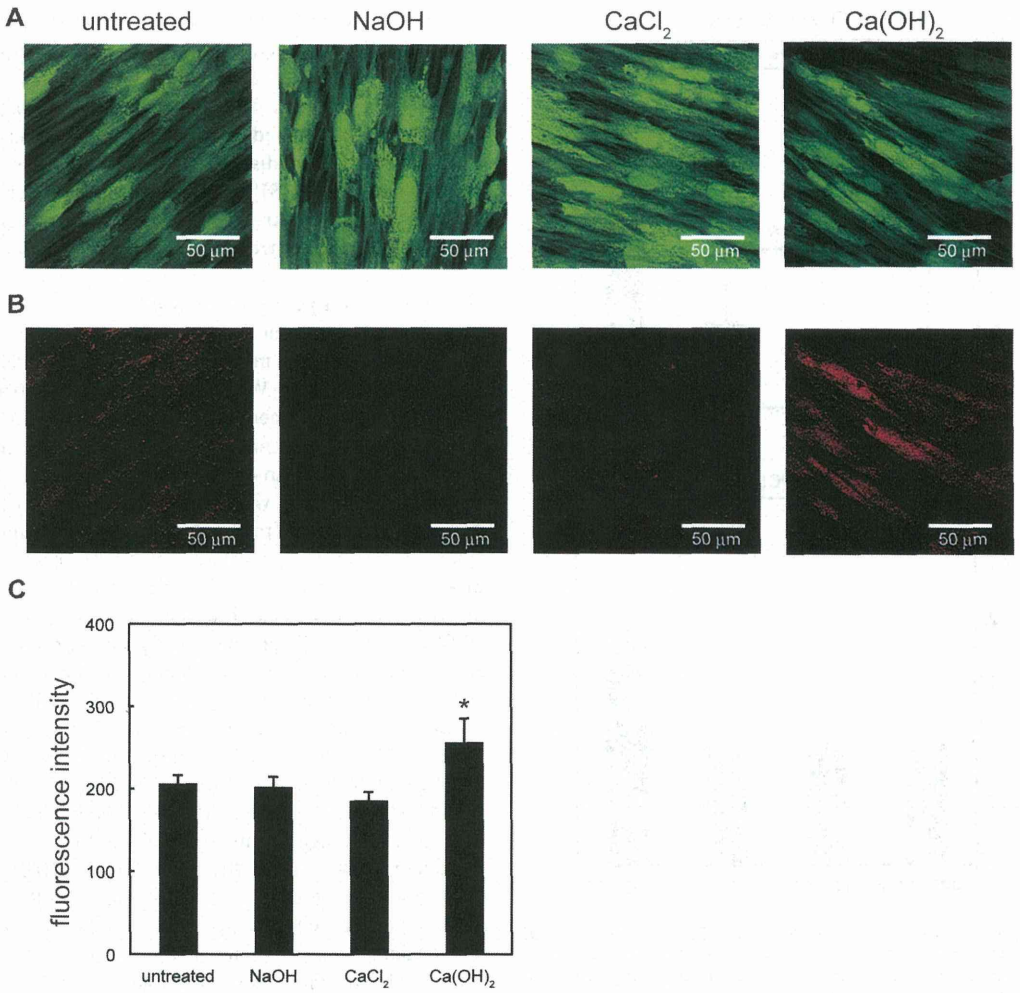


**FIGURE 4.** Confocal microscopy of hMSCs (A) and osteocalcin in hMSCs (B) cultured on chemically modified titanium disks for 28 days. Green: CellTrackerTM Green Fluorescent Probe; red: Alexa Fluor 647 donkey anti-mouse. Images representative of three independent experiments are shown. Fluorescence intensity of osteocalcin in cells on five random areas was measured with the microscope software (B) (FV10-ASW, Olympus). Significant differences versus cells on untreated titanium are shown as $*p < 0.05$.

expression of the osteogenic promoter WNT and its cell surface receptor Frizzled. Furthermore, NaOH treatment induced expression of Axin and adenomatous polyposis coli (APC), scaffold proteins that bind to intracellular Wnt/β-catenin signaling molecules. The receptor activator of nuclear factor-kappaB ligand (RANKL) decoy receptor osteoprotegerin (OPG) was upregulated by NaOH treatment (Fig. 5). $CaCl_2$ treatment induced expression of Frizzled, Axin, APC, and osteogenic markers BMP and IGF-1. Bone matrix protein OPN expression was upregulated by $CaCl_2$ treatment. Expression of integrin β3 was also induced following OPN upregulation by $CaCl_2$ (Fig. 6). $Ca(OH)_2$ treatment induced LRP5/6 and essential coreceptors of Wnt ligands for canonical β-catenin-dependent signal transduction, in addition to WNT, Frizzled, Axin, and APC. RANKL, which functions as a key factor for osteoclast differentiation and activation, was induced by $Ca(OH)_2$, in addition to BMP, IGF-1, and integrin β3. OCN expression was also upregulated by $Ca(OH)_2$ (Fig. 7).

## DISCUSSION

The surface characteristics and chemical composition of titanium are critical in determining biocompatibility. The topography of titanium affects protein adsorption[1,2] and cell–material interactions and regulates osteointegration.[12,23,24,37,38] In this study, we evaluated the influence of chemically modified titanium surface topography on the incorporation of calcium ions on osteogenic differentiation in hMSCs. Sodium hydrogen titanate is formed on the titanium surface by alkali (NaOH) treatment; subsequently, apatite formation is initiated on the chemically treated surface when it is soaked in simulated body fluid.[18,19] Apatite formation is slightly improved on titanium surfaces treated with $CaCl_2$ after NaOH treatment to incorporate calcium ions into the surface.[26] Therefore, we focused on calcium ion incorporation into the titanium surface and investigated the influence of that modification on hMSC differentiation toward an

**TABLE I. Significantly Upregulated Genes in Cells Grown on NaOH-Treated Titanium Disks (Top 30)**

| Symbol | Entrez Gene Name | Fold Change |
|---|---|---|
| TFPI2 | Tissue factor pathway inhibitor 2 | 4.990 |
| PTGS1 | Prostaglandin-endoperoxide synthase 1 (prostaglandin G/H synthase and cyclooxygenase) | 4.821 |
| CXCL6 | Chemokine (C-X-C motif) ligand 6 (granulocyte chemotactic protein 2) | 4.387 |
| PRSS1/PRSS3 | Protease, serine, 1 (trypsin 1) | 4.290 |
| SERPINB2 | Serpin peptidase inhibitor, clade B (ovalbumin), member 2 | 3.989 |
| IL6R | Interleukin 6 receptor | 3.612 |
| PAPPA | Pregnancy-associated plasma protein A, pappalysin 1 | 3.434 |
| AOX1 | Aldehyde oxidase 1 | 3.223 |
| CSGALNACT 1 | Chondroitin sulfate N-acetylgalactosaminyltransferase 1 | 3.197 |
| YTHDC1 | YTH domain containing 1 | 3.169 |
| GPR56 | G protein-coupled receptor 56 | 3.155 |
| OASL | 2′-5′-Oligoadenylate synthetase-like | 3.091 |
| C10orf18 | Family with sequence similarity 208, member B | 3.056 |
| ITGB1 | Integrin, beta 1 (fibronectin receptor, beta polypeptide, antigen CD29 includes MDF2, MSK12) | 2.996 |
| HIST1H2BD | Histone cluster 1, H2bd | 2.992 |
| GALNTL2 | UDP-N-acetyl-alpha-D-galactosamine:polypeptide N-Acetylgalactosaminyltransferase-like 2 | 2.911 |
| IL17RC | Interleukin 17 receptor C | 2.892 |
| TNFSF13B | Tumor necrosis factor (ligand) superfamily, member 13b | 2.736 |
| FAM65B | Family with sequence similarity 65, member B | 2.655 |
| RIN3 | Ras and Rab interactor 3 | 2.653 |
| CCL2 | Chemokine (C-C motif) ligand 2 | 2.647 |
| FRAT1 | Frequently rearranged in advanced T-cell lymphomas | 2.645 |
| CENPM | Centromere protein M | 2.634 |
| TPD52 | Tumor protein D52 | 2.624 |
| TNFSF15 | Tumor necrosis factor (ligand) superfamily, member 15 | 2.597 |
| SFTPA2 | Surfactant protein A2 | 2.574 |
| NR4A2 | Nuclear receptor subfamily 4, group A, member 2 | 2.571 |
| IFI6 | Interferon, alpha-inducible protein 6 | 2.567 |
| SMCHD1 | Structural maintenance of chromosomes flexible hinge domain containing 1 | 2.541 |
| PLCL2 | Phospholipase C-like 2 | 2.488 |

osteogenic lineage. We also compared calcium ion modification by $CaCl_2$ and $Ca(OH)_2$.

Experimental titanium disks were treated with aqueous NaOH, $CaCl_2$, and $Ca(OH)_2$ solutions. hMSC morphology was altered and proliferation was significantly reduced by calcium surface treatment of titanium disks [Fig. 2(A,B)]. Several studies have demonstrated a link between cell shape and osteogenic differentiation in hMSCs.[39–42] In addition, incorporation of calcium ions and apatite formation on the titanium surface treated with $Ca(OH)_2$ were significantly greater than on $CaCl_2$-treated titanium disks [Fig. 1(B,C)]. To investigate the osteogenic differentiation of hMSCs cultured on chemically modified titanium disks, the expression of structural genes for the bone matrix OPN and the marker of bone formation OCN and OCN protein expression were examined (Figs. 3 and 4). OPN transcription in hMSCs was significantly upregulated by the calcium surface treatment, and was significantly on $Ca(OH)_2$-treated disks than on $CaCl_2$-treated disks. OCN protein expression was also upregulated by $Ca(OH)_2$ treatment; however, $CaCl_2$ treatment had no effect on the transcript and protein expression of OCN. We conclude that calcium surface treatment of the titanium disks influenced the osteogenic differentiation of hMSCs, and $Ca(OH)_2$ treatment of the titanium surface induced osteogenic differentiation, whereas $CaCl_2$ treatment had a limited effect.

To investigate the mechanism of osteogenic induction in hMSCs by calcium ions, comparative gene expression profiles were assessed by DNA microarray and pathway analyses. Several genes involved in osteogenic differentiation and bone metabolism were significantly upregulated by the chemical modifications of titanium. IL6R and ITGB1 were significantly upregulated by NaOH (Table I). SPP1 (OPN), MMP13, and ENPP1 were significantly upregulated by $CaCl_2$ and $Ca(OH)_2$ (Tables II and III). $Ca(OH)_2$ treatment also significantly upregulated the expression of IL6R, ITGA2, BMP2, and PTHLH (Table III). In addition, to differentiate the effect of two kinds of calcium surface treatments on gene expression, we compared $CaCl_2$ and $Ca(OH)_2$ treatments and found that $Ca(OH)_2$ treatment significantly upregulated expression of BMP2, PTGS2 (Cox2), PTHLH, and SPP1 (OPN) in hMSCs (Table IV). Previous studies have demonstrated Cox2 function is essential for bone formation in rats[43] and osteoblast differentiation is stimulated through induction of Cox2 in